

Emission properties of a driven artificial atom: increased coherent scattering and off-resonant sideband narrowing

Dara P. S. McCutcheon^{1,*} and Ahsan Nazir^{1,†}

¹*Blackett Laboratory, Imperial College London, London SW7 2AZ, UK*

(Dated: August 24, 2012)

We study the first order field correlation function and emission spectrum of a driven artificial atom. Focusing on the experimentally relevant example of a semiconductor quantum dot, we find that the solid-state (phonon) environment can have a profound effect on the emission characteristics of such a system. For resonant driving, we find an increase in the coherently emitted radiation field with increasing driving strength due to the quantum nature of the phonon bath. This feature is in stark contrast to the standard quantum optics treatment, which predicts a decrease in the fraction of coherent emission with increasing driving strength, and should be observable in experimentally achievable regimes. For off-resonant driving, we show how narrowing in the spectral sideband width can occur in certain regimes, consistent with a known experimental trend.

As described by Mollow, the temporal correlations and fluorescence spectrum of light scattered from a driven two-level system depend crucially on the relative size of the driving strength and the two-level system radiative decay rate [1]. At weak driving strengths, the light is predominately coherently (or elastically) scattered, resulting in the absence of oscillations in the first-order field correlation function, and a single peak in the emission spectrum at the driving laser frequency. At larger driving strengths, however, the coherently scattered light is strongly suppressed, and the emission becomes dominated by incoherently scattered light. This results in oscillations in the field correlation function and a triple-peak structure in the spectrum, known as the Mollow triplet.

While these fundamental predictions have long been confirmed in the traditional quantum optical setting of driven atoms [2], they have only much more recently been observed in solid-state artificial atoms such as driven semiconductor quantum dots (QDs) [3–9], single molecules [10], and superconducting circuits [11]. In fact, in the particular case of QDs, many of the archetypal features of atomic quantum optics have now been seen, such as resonance fluorescence [3–9], coherent population oscillations [6, 12–14], photon anti-bunching [15, 16], and two-photon interference [17–19]. Aside from being of fundamental interest, these observations constitute significant progress towards the ultimate goal that QDs may be used as efficient single photon sources [20–23], and for other quantum technologies [24].

Though a driven QD thus bears a great deal of resemblance to the more idealised case of a driven atom in free space, it is nevertheless unavoidably coupled to its surrounding solid-state environment. For ground-state excitonic transitions in typical InAs QDs, coupling to acoustic phonons has been demonstrated to dominate the QD-environment interaction [13, 14]. This causes the behaviour of the QD, and hence also of its emission properties, to deviate from the atomic case. In particular, a

now well-known signature of phonon coupling is the appearance of an excitation-induced dephasing contribution which depends on the square of the Rabi frequency, with a rate $\gamma \sim \Omega^2$ [8, 13, 14, 25]. This driving dependence is theoretically understood as resulting from phonons that induce transitions between the dressed states of the QD at the Rabi energy [25–28], making it the relevant energy scale in the three-dimensional phonon environment.

Thus, to accurately describe the emission properties of a driven QD, one must faithfully include its coupling to phonons. This can be achieved in various ways, such as through master equations of weak-coupling [25, 26], polaron [28–31], and variational type [32], as well as by several numerical methods [27, 33, 34]. For our purposes, master equation techniques are particularly attractive since, with use of the quantum regression theorem [35], they can readily be extended to investigate field correlation properties. For example, in Refs. [30, 31] a polaron master equation was used to explore the incoherent spectrum of a QD in a micro-pillar cavity, while QD emission under both pulsed [36, 37] and incoherent [38] excitation has also recently been studied.

Here, we extend the variational method of Ref. [32] to explicitly investigate phonon effects in both the coherent and incoherent emission properties of a QD, driven on and off resonance. On resonance - and in stark contrast to the atomic case - we find that at moderate driving the coherent contribution to the QD resonance fluorescence can actually increase with driving strength. This results from an imbalance of phonon absorption and emission processes at low temperatures, an effect that arises naturally in our microscopic model of the phonon bath, but cannot be captured by a simpler treatment in terms of a phenomenological pure dephasing process. We also find that, in an appropriate parameter regime, our model predicts a narrowing of the Mollow sidebands as the QD-laser detuning is increased, which is consistent with recent (and as yet unexplained) experimental observations [8].

Methods summary - We model the QD as a two-level

system with ground state $|0\rangle$ and excited (single exciton) state $|X\rangle$, split by an energy $\hbar\omega_0$. The dot is coherently driven by a laser of frequency ω_l , with Rabi frequency Ω , and is coupled to two separate harmonic oscillator baths to account for both phonon interactions and spontaneous emission into the radiation field. After moving into a frame rotating at frequency ω_l , and making a rotating wave approximation on the driving term, our Hamiltonian takes the form (for $\hbar = 1$)

$$H = \nu |X\rangle\langle X| + \frac{\Omega}{2} \sigma_x + \sum_{\mathbf{k}} \omega_{\mathbf{k}} b_{\mathbf{k}}^\dagger b_{\mathbf{k}} + \sum_{\mathbf{q}} \eta_{\mathbf{q}} a_{\mathbf{q}}^\dagger a_{\mathbf{q}} \\ + |X\rangle\langle X| \sum_{\mathbf{k}} g_{\mathbf{k}} (b_{\mathbf{k}}^\dagger + b_{\mathbf{k}}) + \sum_{\mathbf{q}} (h_{\mathbf{q}} a_{\mathbf{q}} e^{i\omega_l t} \sigma_+ + \text{H.c.}),$$

where $\nu = \omega_0 - \omega_l$ is the QD-laser detuning, $\sigma_+ = |X\rangle\langle 0|$ ($\sigma_- = \sigma_+^\dagger$), $\sigma_x = \sigma_+ + \sigma_-$, and H.c. stands for the Hermitian conjugate. The phonon bath is represented by the creation (annihilation) operators $b_{\mathbf{k}}^\dagger$ ($b_{\mathbf{k}}$) for modes with frequency $\omega_{\mathbf{k}}$, and couples to the QD through the constants $g_{\mathbf{k}}$. The photon bath is similarly defined, with operators $a_{\mathbf{q}}^\dagger$ ($a_{\mathbf{q}}$), frequencies $\eta_{\mathbf{q}}$, and coupling constants $h_{\mathbf{q}}$.

Obtaining an equation of motion for the QD degrees of freedom can be achieved by several means. As mentioned previously, in this work we opt to use the variational master equation method of Ref. [32], since it has been shown to be unrestricted to either weak phonon coupling, or to the small driving limit of polaron theory [28]; it therefore constitutes a robust yet efficient way in which to include the effects of phonons within the QD dynamics. In brief, the variational master equation is derived by first applying a unitary (QD state-dependent) displacement transformation to the full QD-phonon Hamiltonian, which is subsequently optimised on the basis of free-energy minimisation arguments [39]. The second-order, time-local projection operator technique is then used to approximate the QD dynamics in the transformed representation. For our present purposes, the great advantage of using a combination of the quantum regression theorem and a master equation obtained in this way, is that the Born approximation on which the regression theorem relies [35] is performed in a transformed frame, and is not therefore restricted to weak phonon coupling. Full details of the derivation - extended in this work to include the photon bath - can be found in the Appendix.

We find that the Schrödinger picture master equation takes the form

$$\dot{\rho}_V = -\frac{i}{2} [\epsilon \sigma_z + \Omega_r \sigma_x, \rho_V] + \mathcal{K}_{\text{ph}}(\rho_V) + \mathcal{K}_{\text{sp}}(\rho_V), \quad (1)$$

where ρ_V is the reduced density operator for the QD two-level-system in the transformed frame, ϵ is the detuning of the laser from the variationally shifted QD transition frequency, $\Omega_r = \Omega \exp[-\frac{1}{2} \int_0^\infty J_{\text{ph}}(\omega) \omega^{-2} F(\omega)^2 \coth(\beta\omega/2) d\omega]$

is the phonon-renormalised Rabi frequency, with $\beta = 1/k_B T$ the inverse temperature, and $\mathcal{K}_{\text{sp}}(\rho_V) = \Gamma_1 (\sigma_- \rho_V \sigma_+ - (1/2) \{ \sigma_+ \sigma_-, \rho_V \})$ accounts for spontaneous emission processes at a rate Γ_1 . The function $J_{\text{ph}}(\omega) = \sum_{\mathbf{k}} g_{\mathbf{k}}^2 \delta(\omega - \omega_{\mathbf{k}})$ is the QD-phonon spectral density, which for coupling to acoustic phonons is adequately described by $J_{\text{ph}}(\omega) = \alpha \omega^3 \exp[-(\omega/\omega_c)^2]$, with coupling constant α and cut-off frequency ω_c [13, 14]. The factor $F(\omega)$ arises from the variational transformation used in deriving Eq. (1), becoming unity in the full polaron limit. The term $\mathcal{K}_{\text{ph}}(\rho_V)$ contains all phonon effects other than those included in the renormalised Rabi frequency Ω_r , and in general has a fairly complicated form, representing the various processes induced by phonon interactions (e.g. pure-dephasing and phonon emission/absorption). We shall see below, however, that in certain regimes its dominant effects can be approximated by simple intuitive forms.

Though Eq. (1) describes the QD excitonic degrees of freedom, by relating the field operators to those of the QD it can be used to calculate the steady-state first order field correlation function of the QD emission, $g^{(1)}(\tau) = \lim_{t \rightarrow \infty} \langle \sigma_+(t) \sigma_-(t + \tau) \rangle$ [35]. Importantly, $g^{(1)}(\tau)$ does not necessarily approach zero as $\tau \rightarrow \infty$, and in this limit gives the coherent contribution: $g_{\text{coh}}^{(1)} = \lim_{\tau \rightarrow \infty} g^{(1)}(\tau)$. The coherent contribution can be shown to be equal to the square modulus of the off-diagonal elements of the QD density operator in the steady-state, $g_{\text{coh}}^{(1)} = |\rho_{0X}|^2$, and is thus a direct consequence of non-vanishing coherences in the QD. The difference between the full correlation function and the coherent part is then the incoherent component, $g_{\text{inc}}^{(1)}(\tau) = g^{(1)}(\tau) - g_{\text{coh}}^{(1)}$. Armed with the first order field correlation function, we may then calculate the QD emission spectrum, $S(\omega) \propto (1/\pi) \text{Re}[\int_0^\infty e^{i(\omega - \omega_l)\tau} g^{(1)}(\tau) d\tau]$.

Enhanced coherent scattering - We begin our analysis by investigating the emission properties of the QD when driven on resonance with the polaron shifted transition frequency ($\delta = \nu - \sum_{\mathbf{k}} g_{\mathbf{k}}^2 \omega_{\mathbf{k}}^{-1} = 0$). We are interested in examining the detailed effects induced by the coupling to phonons as the driving strength is varied. In particular, we would like to explore deviations from the more phenomenological treatment of environmental interactions (beyond radiative decay) as giving rise simply to sources of pure dephasing [35]. As mentioned, the particular form of $\mathcal{K}_{\text{ph}}(\rho_V)$ already tells us that in general phonon coupling should have an effect on the QD emission properties beyond the pure dephasing model. However, it is instructive to first consider to what extent these effects can be captured by simpler terms in the master equation. For example, at weak driving strengths ($\beta\Omega \ll 1$) we find that we may indeed approximate the phonon influence by a pure dephasing form (see Appendix for details), $\mathcal{K}_{\text{ph}}(\rho_V) \approx (1/2) \gamma_{\text{PD}} (\sigma_z \rho_V \sigma_z - \rho_V)$ in Eq. (1), with a rate given by the expression from polaron theory, $\gamma_{\text{PD}} = (\Omega_r/2)^2 \int_{-\infty}^\infty \cos(\Omega_r s) (e^{\phi(s)} - e^{-\phi(s)}) ds$, where

$\phi(s) = \int_0^\infty J(\omega)\omega^{-2}(\cos(\omega s)\coth(\beta\omega/2) - i\sin(\omega s))d\omega$, and $F(\omega) \rightarrow 1$ in Ω_r [28, 30]. Thus, at sufficiently weak driving strengths, we find that phonon interactions can be represented simply as fluctuations in the excited state energy of the QD, and as such give rise only to an additional pure-dephasing process, consistent with experimental results in this regime [4, 6, 8, 13, 14]. With the further (minor) approximation that $\epsilon = 0$ in Eq. (1), we then arrive at an analytic expression for the first-order field correlation function of a QD interacting with acoustic phonons, in the weak-driving limit:

$$g_{\text{inc}}^{(1)}(\tau) = \frac{\Omega_r^2}{2\Omega_r^2 + 2\Gamma_1\Gamma_2} \times \left[\frac{1}{2}e^{-\Gamma_2\tau} + e^{-\frac{1}{2}(\Gamma_1+\Gamma_2)\tau}(N\cos(\zeta\tau) - M\sin(\zeta\tau)) \right], \quad (2)$$

where $\Gamma_2 = \frac{1}{2}\Gamma_1 + \gamma_{\text{PD}}$, $\zeta = \sqrt{\Omega_r^2 - (1/4)(\Gamma_1 - \Gamma_2)^2}$, $N = (\Omega_r^2 - \Gamma_1(\Gamma_1 - \Gamma_2))/(2\Omega_r^2 + 2\Gamma_1\Gamma_2)$, and $M = (\Omega_r^2(\Gamma_2 - 3\Gamma_1) + \Gamma_1^3\Gamma_2^2(\Gamma_1^{-1} - \Gamma_2^{-1})^2)/(4\zeta(\Omega_r^2 + \Gamma_1\Gamma_2))$. The coherent contribution in this limit is given by

$$g_{\text{coh}}^{(1)} = \left(\frac{\Gamma_1\Omega_r}{2\Gamma_1\Gamma_2 + 2\Omega_r^2} \right)^2, \quad (3)$$

which would clearly approach zero if Ω_r were allowed to become large.

Eqs. (2) and (3) are essentially the standard atomic $g^{(1)}(\tau)$ expressions, when extended to include pure-dephasing [4, 6]. The only difference here is that we explicitly include a *driving dependent* pure-dephasing rate through γ_{PD} , and that the driving is itself renormalised by the phonon environment through Ω_r . Both of these features are important for these expressions to adequately approximate the full dynamics. For weak exciton-phonon coupling, we can expand the exponential factors in the pure-dephasing rate to further approximate as $\gamma_{\text{PD}} \approx \frac{\pi}{2}J(\Omega_r)\coth(\beta\Omega_r/2)$, which for $\beta\Omega \ll 1$ and $\Omega_r/\omega_c \ll 1$ takes on the well known form $\gamma_{\text{PD}} \sim \Omega_r^2$ [13, 14, 25, 28]. In the frequency domain, this form of pure-dephasing will be apparent in the broadening of the spectral sidebands with increasing driving strength [8, 30, 31].

Thus, at weak driving, phonon coupling does not induce behaviour markedly different from the atomic case. However, to exemplify the breakdown of the pure-dephasing model at stronger driving strengths, in Fig. 1 we plot $g^{(1)}(\tau)$ calculated using the full variational theory (solid blue curves) and calculated using Eqs. (2) and (3) (black dashed curves). As expected, for low driving strengths, $\Omega < 0.1\text{ps}^{-1}$ ($< 15\text{GHz}$ in linear frequency) the pure-dephasing model gives an excellent approximation to the full theory. As the driving strength is increased, however, significant discrepancies soon begin to become apparent. In particular, from the different long-time values that are approached when $\Omega \geq 0.33\text{ps}^{-1}$,

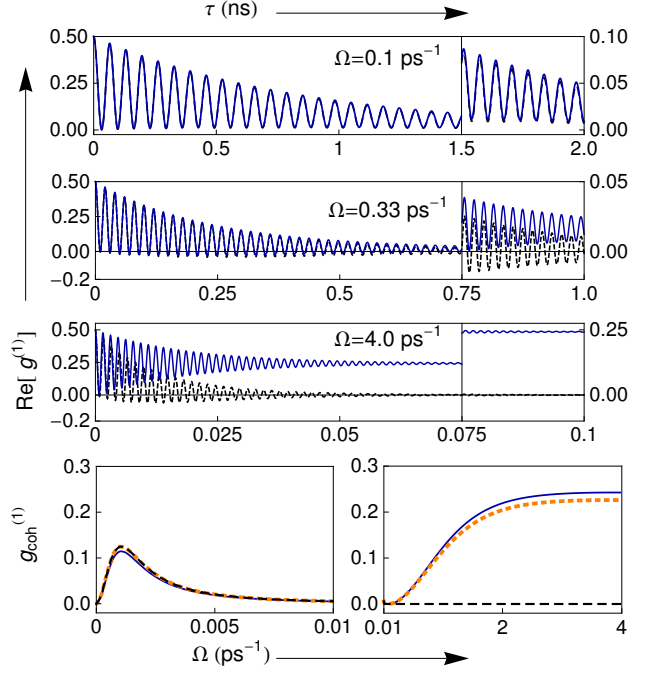


FIG. 1: First order field correlation function for various driving strengths as indicated, calculated using the full variational theory (blue solid curves), and calculated using the pure-dephasing approximation of Eqs. (2) and (3) (black dashed curves). The right-most parts of the upper three plots show enlargements of the long-time behaviour. The lower plots show only the coherent contribution, now as a function of driving strength, calculated using the same methods as in the other plots, and also from the simple expression of Eq. (4) (orange dotted curve). The lower left plot shows the only region where the pure-dephasing model gives a non-negligible coherent contribution, close to the origin. Parameters: $T_1 = 700\text{ps}$, $\alpha = 0.027\text{ps}^2$, $\omega_c = 2.2\text{ps}^{-1}$, and $T = 4\text{K}$.

we can conclude that the coherent contribution begins to become important, and that this is not captured by the pure-dephasing approximation. Indeed, when $\Omega = 4\text{ps}^{-1}$ we see that in the full phonon theory a long-time limit of $g_{\text{coh}}^{(1)} \sim 0.25$ is approached, in clear distinction to the pure-dephasing model.

That Eqs. (2) and (3) cannot capture these effects signifies that above a driving strength of $\Omega \sim 0.1\text{ps}^{-1}$ (for these realistic parameters), the field correlation properties of the QD emission fundamentally depart from the atomic case. This departure can be attributed to phonon-induced coherences in the steady-state of the QD. The pure dephasing model is unable to capture this effect, as it does not lead to the correct equilibration with respect to the phonon bath; it essentially assumes an infinite temperature limit, and thus the quantum nature of the environment is lost. However, for resonant driving, we may still approximate this process in a simple way, by modifying the phonon term in Eq. (1) to $\mathcal{K}_{\text{ph}}(\rho_V) \approx (1/2)\gamma_{\text{PD}}(\sigma_z\rho_V\sigma_z - \rho_V) + (i/4)\kappa[\sigma_y, \{\sigma_z, \rho_V\}]$,

where $\kappa = (\Omega_r/2)^2 \int_{-\infty}^{\infty} \sin(\Omega_r s) (e^{\phi(s)} - e^{-\phi(s)}) ds$, such that $\kappa/\gamma_{PD} = \tanh(\beta\Omega_r/2)$ [28]. With this adjustment both contributions to $g^{(1)}(\tau)$ depart from the atomic case [41]. Specifically, the coherent contribution now becomes

$$G_{\text{coh}}^{(1)} = \left(\frac{\Gamma_1 \Omega_r}{2\Gamma_1 \Gamma_2 + 2\Omega_r^2} \right)^2 + \left(\frac{B\kappa}{\Gamma_1 + 2\gamma_{PD}} \right)^2, \quad (4)$$

where $B = \Omega_r/\Omega$ is the renormalisation factor, arising here since we must transform out of the variational frame to obtain the QD coherences.

We see that the coherent contribution now has two terms. The first, which was present in the pure-dephasing model, has a maximum when $\Omega_r = \sqrt{\Gamma_1 \Gamma_2}$, but quickly tends to zero as Ω_r is increased. The second term is present nowhere in the standard quantum optical treatment and becomes important for larger values of Ω_r . In fact, once the driving is strong enough such that $\Gamma_1 \ll \gamma_{PD}$, we can approximate $G_{\text{coh}}^{(1)} \approx (B \tanh(\beta\Omega_r/2)/2)^2$. Thus, with reference to Fig. 1, we see that at a temperature of 4 K, we have $k_B T \approx 0.5 \text{ ps}^{-1}$, and when driving at $\Omega = 0.1 \text{ ps}^{-1}$ we are still effectively in a high temperature regime ($\beta\Omega < 1$). As such, the coherent contribution arising from the QD-phonon coupling is unimportant, and the pure-dephasing approximation is adequate. As the driving is increased, however, the quantum nature of the phonon environment begins to play an increasingly important role, and the coherent contribution is enhanced correspondingly. When the driving becomes very large, the coherent contribution saturates at around $B^2/4$ [42]. These observations are borne out in the lower part of Fig. 1, where the coherent contribution is plotted as a function of Ω using the full variational theory together with the approximate expression of Eq. (4), which captures the general trend, though gives a slight underestimate at large driving. The lower left plot shows the region close to the origin, the *only regime* in which the pure-dephasing model gives a non-negligible coherent contribution.

Spectrum - Having investigated the behaviour of the coherent contribution to the QD emission, we now turn our attention to the properties of the QD emission spectrum. We shall now concentrate on the regime where the incoherent contribution dominates (i.e. relatively weak driving), and Eq. (2) is thus approximately valid on resonance. From a Fourier transform of Eq. (2), we find that the resonant Mollow sideband widths are determined by $\Gamma_1 + \Gamma_2 = (3/2)\Gamma_1 + \gamma_{PD}$, while their positions are given approximately by $\pm\Omega_r$. As such, we expect them to show a systematic broadening and splitting with increasing driving strength, as has already been confirmed [8, 30]. Off resonance, we might then also expect sideband broadening and splitting with increasing *detuning* (for fixed Ω) if we were to replace Ω_r with the generalised Rabi frequency, $\Omega'_r = \sqrt{\Omega_r^2 + \delta^2}$ [8]. This would lead to similar

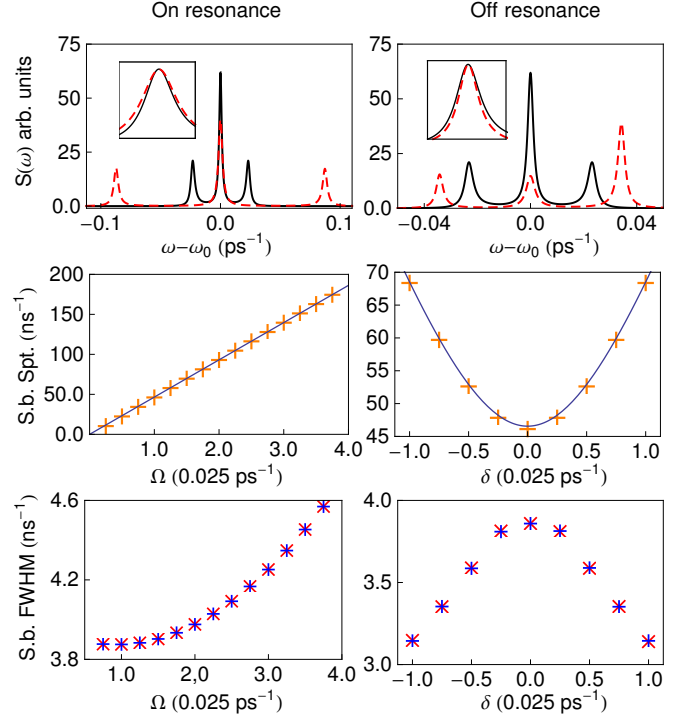


FIG. 2: From top to bottom, incoherent emission spectrum, extracted sideband splitting, and extracted sideband width for varying driving strengths on resonance (left), and varying detunings (right). The solid black curves in the emission spectra are for $\delta = 0$, and a driving strength of $\Omega = 0.025 \text{ ps}^{-1}$ (which sets our x-axis units in the rest of the plots). The dashed red curves are for $\Omega = 0.094 \text{ ps}^{-1}$ on resonance, and $\delta = \Omega = 0.025 \text{ ps}^{-1}$ off resonance (which has been enhanced by a factor of 5). The insets in each case show the red sidebands shifted and rescaled to lie on top of each other. The solid blue curves in the middle row show the functions $2\Omega_r$ (left) and $2\sqrt{\Omega_r^2 + \delta^2}$ (right). The symbols in the bottom row correspond to the red (x) and blue (+) sidebands. Parameters: $T_1 = 400 \text{ ps}$, $\alpha = 0.027 \text{ ps}^2$, $\omega_c = 2.2 \text{ ps}^{-1}$, and $T = 10 \text{ K}$.

trends for increasing δ as for Ω . However, the experiments of Ref. [8] showed a systematic *narrowing* of the Mollow sidebands with increasing detuning, despite the fact that the splitting is well captured by a generalised Rabi frequency of a form similar to Ω'_r , leaving open the question as to why this might be the case.

In fact, off-resonance, the expressions for the spectrum become significantly more complicated than in the resonant case, and the above simple reasoning does not hold. To illustrate this, in Fig. 2, from top to bottom, we plot the incoherent emission spectrum, extracted sideband splitting, and extracted full-width-half-maximum ($= \Gamma$) of the Mollow sidebands, calculated from the full phonon theory. In the latter two cases, the spectrum was fitted to a sum of three model Lorentzian functions of the form $L(\omega) = 0.5\Gamma/[(\omega - \omega_p)^2 + (0.5\Gamma)^2]$. The left column corresponds to varying the driving frequency on resonance,

while the right column corresponds to varying the detuning with a fixed driving strength. For the spectra in the top row, the black solid curves both correspond to driving at a strength $\Omega = 0.025 \text{ ps}^{-1}$ on resonance, while the red dashed curve on the left corresponds to increasing the driving strength up to $\Omega = 0.094 \text{ ps}^{-1}$, and that on the right has values of $\delta = \Omega = 0.025 \text{ ps}^{-1}$. Before any detailed analysis is performed, from the shape of these two emission spectra, it is evident that moving off-resonance is not equivalent to increasing the driving strength; the asymmetry in the off-resonant case cannot be captured by any combination of parameters in the resonant case.

A more detailed analysis of the spectra reveals two important trends. Firstly, as can be seen by the sideband splittings in the middle row, increasing the driving strength on resonance does, as expected, cause the sidebands to move apart linearly with Ω . Also, we see that moving off-resonance appears to alter the sideband splitting in exact accordance with the simple procedure of replacing $\Omega_r \rightarrow \sqrt{\Omega_r^2 + \delta^2}$. The extracted sideband widths in the lower row, however, reveal something quite different. On the left we plot the extracted sideband widths as a function of driving strength on resonance. In accordance with our approximate pure-dephasing model, for which we have $\gamma_{\text{PD}} \sim \Omega_r^2$, we see a systematic broadening of the sidebands with increasing driving strength. On the lower right, we plot the extracted widths of the red (red crosses) and blue (blue crosses) sidebands as a function of detuning. In contrast, we now see a systematic *narrowing* of the sidebands [43], consistent with recent experimental results [8]. To further confirm this point, the insets of the plots in the top row show the red sidebands in each case plotted on top of each other. It is important to note that, while we have attempted to model neither the effects of the cavity in Ref. [8], which can be significant [30, 31], nor other sources of noise beyond phonons, these results still demonstrate that an increase in sideband splitting off-resonance does not necessarily lead to an associated phonon-induced increase in sideband width.

We can gain some approximate analytical insight into this behaviour by again considering the pure-dephasing limit. Allowing for off-resonant driving, we expand the sideband widths to second order in the detuning, from which we find that they are now determined by $(3/2)\Gamma_1 + \gamma_{\text{PD}} - (\delta/\sqrt{2}\Omega_r)^2(\Gamma_1 - 2\gamma_{\text{PD}})$. Hence, for $\Gamma_1 > 2\gamma_{\text{PD}}$, as is the case in Fig. 2, we expect narrowing with increasing detuning from resonance. Finally, it is also worth noting that the pure dephasing rate is itself modified off-resonance, and becomes $\gamma_{\text{PD}} \approx \frac{\pi}{2} \frac{\Omega_r^2}{\Omega_r'^2} J(\Omega_r') \coth(\beta\Omega_r'/2)$ in the weak-coupling limit. For our cubic spectral density, we then find $\gamma_{\text{PD}} \sim \alpha\Omega_r'^2 \exp[-\Omega_r'^2/\omega_c^2]$ for low temperatures ($\beta\Omega_r' \gg 1$) which increases with detuning for $\Omega_r' \ll \omega_c$. On the other hand, at high temperatures ($\beta\Omega_r' \ll 1$) we have $\gamma_{\text{PD}} \sim \alpha(\Omega_r'^2/\beta) \exp[-\Omega_r'^2/\omega_c^2]$, which *decreases* with increasing detuning, though slowly

for $\Omega_r' \ll \omega_c$. This is the relevant regime for Fig. 2.

In summary, we have studied the coherent and incoherent contributions to the first order field correlation function and emission spectrum of a driven artificial atom, focusing on the role played by the solid-state (phonon) environment. For resonant driving, we find an increase in the coherently emitted radiation field with increasing driving strength due entirely to the influence of the phonon bath. This feature is thus absent in the standard quantum optics treatment, which predicts negligible coherently emitted radiation in the same limit. For weak off-resonant driving, we have also shown that despite the fact that the generalised Rabi frequency increases with detuning, phonon interactions do not necessarily lead to a related increase in spectral sideband width. In fact, sideband narrowing can occur in certain regimes, consistent with an observed experimental trend [8]. Though we have concentrated here on the case of a driven QD, the model we have employed is sufficiently general to apply to a wide range of two-level systems in which environmental interactions (beyond spontaneous emission) are significant. We would therefore expect the qualitative features of artificial atom emission that we have outlined above to be observable in various experimental settings.

Acknowledgments - During the completion of this work we became aware of similar results obtained independently for the spectral narrowing, and we would like to thank Stephen Hughes and co-workers for bringing these to our attention. We also thank Clemens Matthiesen, Brendon Lovett, Erik Gauger, and Sean Barrett for fruitful discussions. D.P.S.M. acknowledges support from the EPSRC and CHIST-ERA project SSQN. A.N. thanks Imperial College for support.

* Electronic address: d.mccutcheon@imperial.ac.uk

† Electronic address: a.nazir@imperial.ac.uk

- [1] B. R. Mollow, Phys. Rev. **188**, 1969 (1969).
- [2] F. Schuda, C. R. Stroud Jr, and M. Hercher, J. Phys. B **7**, L198 (1974).
- [3] X. Xu et al., Science **317**, 929 (2007).
- [4] A. Muller et al., Phys. Rev. Lett. **99**, 187402 (2007).
- [5] S. Ates et al., Phys. Rev. Lett. **103**, 167402 (2009).
- [6] E. B. Flagg et al., Nature Phys. **5**, 203 (2009).
- [7] A. N. Vamivakas et al., Nature Phys. **5**, 198 (2009).
- [8] S. M. Ulrich et al., Phys. Rev. Lett. **106**, 247402 (2011).
- [9] A. Ulhaq et al., Nature Photon. **6**, 238 (2012).
- [10] G. Wrigge et al., Nature Phys. **4**, 60 (2008).
- [11] O. Astafiev et al., Science **327**, 840 (2010).
- [12] A. Zrenner et al., Nature **418**, 612 (2002).
- [13] A. J. Ramsay et al., Phys. Rev. Lett. **104**, 017402 (2010).
- [14] A. J. Ramsay et al., Phys. Rev. Lett. **105**, 177402 (2010).
- [15] P. Michler et al., Science **290**, 2282 (2000).
- [16] C. Santori et al., Phys. Rev. Lett. **86**, 1502 (2001).
- [17] C. Santori et al., Nature **419**, 594 (2002).
- [18] E. B. Flagg et al., Phys. Rev. Lett. **104**, 137401 (2010).
- [19] R. B. Patel et al., Nature Photon. **4**, 632 (2010).

- [20] H. S. Nguyen et al., Appl. Phys. Lett. **99**, 261904 (2011).
- [21] C. Matthiesen, A. N. Vamivakas, and M. Atatüre, Phys. Rev. Lett. **108**, 093602 (2012).
- [22] K. Konthasinghe et al., Phys. Rev. B **85**, 235315 (2012).
- [23] A. Kiraz, M. Atatüre, and A. Imamoglu, Phys. Rev. A **69**, 032305 (2004).
- [24] S. Benjamin, B. Lovett, and J. M. Smith, Laser & Photon. Rev. **3**, 556 (2009).
- [25] A. Nazir, Phys. Rev. B **78**, 153309 (2008).
- [26] P. Machnikowski and L. Jacak, Phys. Rev. B. **69**, 193302 (2004).
- [27] A. Vagov et al., Phys. Rev. Lett. **98**, 227403 (2007).
- [28] D. P. S. McCutcheon and A. Nazir, New J. Phys. **12**, 113042 (2010).
- [29] I. Wilson-Rae and A. Imamoglu, Phys. Rev. B **65**, 235311 (2002).
- [30] C. Roy and S. Hughes, Phys. Rev. Lett. **106**, 247403 (2011).
- [31] C. Roy and S. Hughes, Phys. Rev. B **85**, 115309 (2012).
- [32] D. P. S. McCutcheon et al., Phys. Rev. B **84**, 081305(R) (2011).
- [33] J. Förstner et al., Phys. Rev. Lett. **91**, 127401 (2003).
- [34] A. Krugel et al., Appl. Phys. B. **81**, 897 (2005).
- [35] H. J. Carmichael, *Statistical Methods in Quantum Optics* (Springer, New York, 1998).
- [36] K. J. Ahn, J. Förstner, and A. Knorr, Phys. Rev. B **71**, 153309 (2005).
- [37] A. Moelbjerg et al., Phys. Rev. Lett. **108**, 017401 (2012).
- [38] E. del Valle and F. P. Laussy, Phys. Rev. Lett. **105**, 233601 (2010).
- [39] R. Silbey and R. A. Harris, J. Chem. Phys. **80**, 2615 (1984).
- [40] H.-P. Breuer and F. Petruccione, *The Theory of Open Quantum Systems* (Oxford University Press, 2002).
- [41] It is worth mentioning that, in general, this approximation is also too simple to fully capture the field correlation properties, though it gives useful insight into the behaviour of the coherent contribution on resonance.
- [42] Though at driving strengths $\Omega \gg \omega_c$ the system will become decoupled from the phonon environment leading to a decrease in the coherent contribution.
- [43] The central peak shows broadening in the same parameter regime.

APPENDIX

In this Appendix we give the derivation of the master equation used in the main text, Eq. (1). We first show how the quantum dot-phonon and quantum dot-photon effects can be treated independently within our formalism. We then give the resulting expressions of the variational method used to treat the quantum dot-phonon coupling, and shown how they reduce to a pure-dephasing form in the appropriate limit.

The system

We model the quantum dot (QD) as a two-level system with ground-state $|0\rangle$ and excited (single-exciton) state $|X\rangle$, separated by an energy $\hbar\omega_0$. The QD is continuously driven by a laser of frequency ω_l , with Rabi frequency Ω , and is coupled both to a phonon bath, represented by an infinite collection of harmonic oscillators of frequencies $\omega_{\mathbf{k}}$ and creation (annihilation) operators $b_{\mathbf{k}}^\dagger$ ($b_{\mathbf{k}}$), and to the radiation field, again represented by an infinite collection of harmonic oscillators, this time of frequencies $\eta_{\mathbf{q}}$ and creation (annihilation) operators $a_{\mathbf{q}}^\dagger$ ($a_{\mathbf{q}}$). The two baths are assumed to be entirely independent, such that $[a_{\mathbf{q}}, b_{\mathbf{k}}^\dagger] = [b_{\mathbf{k}}, a_{\mathbf{q}}^\dagger] = 0$, etc.

In a frame rotating at the laser frequency, and within the dipole and rotating wave approximation for the QD-radiation field coupling, the complete Hamiltonian has the form (setting $\hbar = 1$)

$$H = \nu|X\rangle\langle X| + \frac{\Omega}{2}\sigma_x + \sum_{\mathbf{k}} \omega_{\mathbf{k}} b_{\mathbf{k}}^\dagger b_{\mathbf{k}} + |X\rangle\langle X| \sum_{\mathbf{k}} g_{\mathbf{k}}(b_{\mathbf{k}}^\dagger + b_{\mathbf{k}}) + \sum_{\mathbf{q}} \eta_{\mathbf{q}} a_{\mathbf{q}}^\dagger a_{\mathbf{q}} + \sum_{\mathbf{q}} (h_{\mathbf{q}} a_{\mathbf{q}} \sigma_+ e^{i\omega_l t} + h_{\mathbf{q}}^* a_{\mathbf{q}}^\dagger \sigma_- e^{-i\omega_l t}), \quad (5)$$

where a rotating-wave approximation has also been made on the driving term. Here, $\nu = \omega_0 - \omega_l$ is the detuning of the laser from the excitonic transition energy, the QD-phonon couplings are denoted by $g_{\mathbf{k}}$ (assumed real) and the QD-radiation field couplings by $h_{\mathbf{q}}$. The Pauli matrices are defined in the usual way, such that $\sigma_x = \sigma_- + \sigma_+ = |0\rangle\langle X| + |X\rangle\langle 0|$ and $\sigma_z = |X\rangle\langle X| - |0\rangle\langle 0|$.

Variational transformation

We now apply a unitary variational transformation to H in order to attempt to treat the QD-phonon interaction beyond the weak coupling approximation [32]. The transformed Hamiltonian is defined by $H_V = e^V H e^{-V}$, where

$$V = |X\rangle\langle X| \sum_{\mathbf{k}} (\alpha_{\mathbf{k}} b_{\mathbf{k}}^\dagger - \alpha_{\mathbf{k}}^* b_{\mathbf{k}}), \quad (6)$$

with $\alpha_{\mathbf{k}} = f_{\mathbf{k}}/\omega_{\mathbf{k}}$, and where $f_{\mathbf{k}}$ are variational parameters to be determined later. We can write $e^{\pm V} = |0\rangle\langle 0| + |X\rangle\langle X| \prod_{\mathbf{k}} D(\pm\alpha_{\mathbf{k}})$ where $\prod_{\mathbf{k}} D(\pm\alpha_{\mathbf{k}}) = \prod_{\mathbf{k}} \exp[\pm(\alpha_{\mathbf{k}} b_{\mathbf{k}}^\dagger - \alpha_{\mathbf{k}}^* b_{\mathbf{k}})]$ is a product of displacement operators $D(\pm\alpha_{\mathbf{k}})$. After the variational transformation, we find $H_V = H_S + H_{1a} + H_{1b} + H_{12} + H_{B_1} + H_{B_2}$, where

$$H_S = \frac{R}{2} \mathbb{1} + \frac{\epsilon}{2} \sigma_z + \frac{\Omega_r}{2} \sigma_x, \quad (7)$$

the interaction terms $H_{1a} = |X\rangle\langle X| \sum_{\mathbf{k}} (g_{\mathbf{k}} - f_{\mathbf{k}})(b_{\mathbf{k}}^\dagger + b_{\mathbf{k}})$ and $H_{1b} = \frac{\Omega}{2}(\sigma_x B_x + \sigma_y B_y)$ contain only QD and phonon operators, the interaction term

$$H_{12} = \sum_{\mathbf{q}} (h_{\mathbf{q}} a_{\mathbf{q}} B_+ \sigma_+ e^{i\omega_l t} + h_{\mathbf{q}}^* a_{\mathbf{q}}^\dagger B_- \sigma_- e^{-i\omega_l t}), \quad (8)$$

contains QD, phonon, and photon operators, and the bath Hamiltonians are $H_{B_1} = \sum_{\mathbf{k}} \omega_{\mathbf{k}} b_{\mathbf{k}}^\dagger b_{\mathbf{k}}$ and $H_{B_2} = \sum_{\mathbf{q}} \eta_{\mathbf{q}} a_{\mathbf{q}}^\dagger a_{\mathbf{q}}$. The detuning is now $\epsilon = \omega'_0 - \omega_l$, defined in terms of the *bath-shifted* QD transition energy $\omega'_0 = \omega_0 + R$, with $R = \sum_{\mathbf{k}} \omega_{\mathbf{k}}^{-1} f_{\mathbf{k}}(f_{\mathbf{k}} - 2g_{\mathbf{k}})$. The bath operators are given by $B_x = \frac{1}{2}(B_+ + B_- - 2B)$ and $B_y = \frac{1}{2i}(B_- - B_+)$, where $B_{\pm} = \prod_{\mathbf{k}} D(\pm\alpha_{\mathbf{k}})$, which have the same average with respect to a thermal equilibrium state of the phonon bath: $B = \langle B_{\pm} \rangle = \exp[-(1/2) \sum_{\mathbf{k}} |\alpha_{\mathbf{k}}|^2 \coth(\beta\omega_{\mathbf{k}}/2)]$, with inverse temperature $\beta = 1/(k_B T)$. The *bath-renormalised* Rabi frequency, which appears in the system-Hamiltonian as a result of our choice of bath operators B_x and B_y , is $\Omega_r = B\Omega$.

Time-local master equation

To proceed with the master equation derivation, let us now separate the variationally-transformed Hamiltonian into interacting and non-interacting terms such that $H_V = H_0 + H_I$, with $H_0 = H_S + H_{B_1} + H_{B_2}$ and $H_I = H_{1a} + H_{1b} + H_{12}$, and treat H_I as a perturbation. Notice that while the interaction terms H_{1a} and H_{1b} depend only on QD and phonon operators, and not on the radiation field, the term H_{12} does not depend solely on QD and radiation field operators, but also on the phonon operators B_{\pm} as a result of the variational transformation. At this stage, we could perform a mean-field-type approximation and replace B_{\pm} by their average B in Eq. (8), which would significantly simplify the form of H_{12} . However, we shall not perform such an approximation here, but instead attempt to account explicitly for the interplay between the phonon and radiation field operators in the following master equation derivation.

We now move into the interaction picture with respect to H_0 , yielding an interaction Hamiltonian in the (variationally-transformed) interaction picture of the form $\tilde{H}_I(t) = \tilde{H}_{1a}(t) + \tilde{H}_{1b}(t) + \tilde{H}_{12}(t)$, where $\tilde{H}_{1a}(t) = e^{iH_0 t} H_{1a} e^{-iH_0 t}$, $\tilde{H}_{1b}(t) = e^{iH_0 t} H_{1b} e^{-iH_0 t}$, and $\tilde{H}_{12}(t) = e^{iH_0 t} H_{12} e^{-iH_0 t}$ (tildes indicate interaction picture operators). We find $\tilde{H}_{1a}(t) = \tilde{\pi}_X(t) \sum_{\mathbf{k}} (g_{\mathbf{k}} - f_{\mathbf{k}}) (b_{\mathbf{k}}^{\dagger} e^{i\omega_{\mathbf{k}} t} + b_{\mathbf{k}} e^{-i\omega_{\mathbf{k}} t})$ with $\tilde{\pi}_X(t) = e^{iH_S t} |X\rangle\langle X| e^{-iH_S t}$, while $\tilde{H}_{1b}(t) = \frac{\Omega}{2} (\sigma_x(t) B_x(t) + \sigma_y(t) B_y(t))$ where $\sigma_n(t) = e^{iH_S t} \sigma_n e^{-iH_S t}$ and $B_n(t) = e^{iH_{B_1} t} B_n e^{-iH_{B_1} t}$ for $n = x, y$. Explicitly, we may write $B_x(t) = \frac{1}{2}(B_+(t) + B_-(t) - 2B)$ and $B_y(t) = \frac{1}{2i}(B_-(t) - B_+(t))$, where $B_{\pm}(t) = e^{iH_{B_1} t} B_{\pm} e^{-iH_{B_1} t} = \prod_{\mathbf{k}} D(\pm\alpha_{\mathbf{k}} e^{i\omega_{\mathbf{k}} t})$. The third term (QD-photon-phonon) is given by

$$\tilde{H}_{12}(t) = \sum_{\mathbf{q}} (h_{\mathbf{q}} a_{\mathbf{q}} e^{-i\eta_{\mathbf{q}} t} B_+(t) \sigma_+(t) e^{i\omega_{\mathbf{q}} t} + h_{\mathbf{q}}^* a_{\mathbf{q}}^{\dagger} e^{i\eta_{\mathbf{q}} t} B_-(t) \sigma_-(t) e^{-i\omega_{\mathbf{q}} t}), \quad (9)$$

where $\sigma_{\pm}(t) = e^{iH_S t} \sigma_{\pm} e^{-iH_S t}$, and $B_{\pm}(t)$ are as defined above. We now consider the products

$$\sigma_{\pm}(t) e^{\pm i\omega_{\mathbf{q}} t} = \exp \left[i \left(\frac{\epsilon}{2} \sigma_z + \frac{\Omega_r}{2} \sigma_x \right) t \right] \sigma_{\pm} \exp \left[-i \left(\frac{\epsilon}{2} \sigma_z + \frac{\Omega_r}{2} \sigma_x \right) t \right] e^{\pm i(\omega_0 - \nu) t} \quad (10)$$

which appear in Eq. (9). Provided that $\omega_0 \gg \nu, \epsilon, \Omega_r$, which is generally the case for driven QDs since $\omega_0 \sim 1$ eV compared to meV or smaller energy scales for the other quantities, then we may approximate $\sigma_{\pm}(t) e^{\pm i\omega_{\mathbf{q}} t} \approx \sigma_{\pm} e^{\pm i\omega_0 t}$, which simplifies the third interaction term to

$$\tilde{H}_{12}(t) \approx \sum_{\mathbf{q}} (h_{\mathbf{q}} a_{\mathbf{q}} e^{-i\eta_{\mathbf{q}} t} B_+(t) \sigma_+ e^{i\omega_0 t} + h_{\mathbf{q}}^* a_{\mathbf{q}}^{\dagger} e^{i\eta_{\mathbf{q}} t} B_-(t) \sigma_- e^{-i\omega_0 t}), \quad (11)$$

without any significant loss of accuracy.

We now follow the standard projection-operator procedure [40] to derive a time-local master equation for the reduced QD exciton density operator, $\tilde{\rho}_V$, in the variational frame interaction picture, treating $\tilde{H}_I(t)$ to second order (the first order term in $\tilde{H}_I(t)$ disappears). In doing so we arrive at the usual expression

$$\frac{d\tilde{\rho}_V(t)}{dt} = - \int_0^t \text{dstr}_B [\tilde{H}_I(t), [\tilde{H}_I(s), \tilde{\rho}_V(t) \rho_B]]. \quad (12)$$

Here, ρ_B is a reference state of the environment (comprising both phonons and the radiation field), which we take to be a thermal equilibrium state: $\rho_B = e^{-\beta H_B} / \text{tr}_B(e^{-\beta H_B}) = [e^{-\beta H_{B_1}} / \text{tr}_{B_1}(e^{-\beta H_{B_1}})] [e^{-\beta H_{B_2}} / \text{tr}_{B_2}(e^{-\beta H_{B_2}})] = \rho_{B_1} \rho_{B_2}$. Inserting $\tilde{H}_I(t) = \tilde{H}_{1a}(t) + \tilde{H}_{1b}(t) + \tilde{H}_{12}(t)$ into Eq. (12) we find that the master equation consists of nine terms corresponding to the different possible combinations of the three interaction terms. However, since $\langle \tilde{H}_{1a} \rangle_{B_1} = \langle \tilde{H}_{1b} \rangle_{B_1} = \langle \tilde{H}_{12} \rangle_{B_2} = 0$, we find that those terms containing \tilde{H}_{1a} or \tilde{H}_{1b} and \tilde{H}_{12} disappear. We are then left with

$$\frac{d\tilde{\rho}_V(t)}{dt} = - \int_0^t \text{dstr}_{B_1} [\tilde{H}_{1a}(t) + \tilde{H}_{1b}(t), [\tilde{H}_{1a}(s) + \tilde{H}_{1b}(s), \tilde{\rho}_V(t) \rho_{B_1}]] - \int_0^t \text{dstr}_{B_1+B_2} [\tilde{H}_{12}(t), [\tilde{H}_{12}(s), \tilde{\rho}_V(t) \rho_{B_1} \rho_{B_2}]]. \quad (13)$$

The first term on the right-hand of Eq. (13) is precisely that expected from the variational treatment of QD exciton-phonon interactions in the absence of the radiation field, and is thus unaffected by the extra coupling to the electromagnetic field. However, the second term, responsible for photon emission and absorption processes due to the radiation field, appears at this stage to be modified by the phonon environment, due to our use of the variational transformation. We shall now show that for typical QD parameters this term should actually reduce to the usual form expected in the absence of phonon interactions.

Spontaneous emission terms

We now write $\frac{d\tilde{\rho}_V(t)}{dt} = \tilde{\mathcal{K}}_{\text{ph}}(\tilde{\rho}_V(t)) + \tilde{\mathcal{K}}_{\text{sp}}(\tilde{\rho}_V(t))$ where

$$\tilde{\mathcal{K}}_{\text{sp}}(\tilde{\rho}_V(t)) = - \int_0^t \text{dstr}_{B_1+B_2} [\tilde{H}_{12}(t), [\tilde{H}_{12}(s), \tilde{\rho}_{SP}(t) \rho_{B_1} \rho_{B_2}]]. \quad (14)$$

and consider this term in more detail. The QD-phonon coupling term $\tilde{\mathcal{K}}_{\text{ph}}(\tilde{\rho}_V(t))$ is discussed later. To proceed, we write $\tilde{H}_{12}(t) = A(t)Q(t)B_+(t) + (A(t)Q(t)B_+(t))^\dagger$, with $A(t) = \sigma_+ e^{i\omega_0 t}$ and $Q(t) = \sum_{\mathbf{q}} h_{\mathbf{q}} a_{\mathbf{q}} e^{-i\eta_{\mathbf{q}} t}$, where $A(t)$, $Q(t)$, and $B_+(t)$ all commute. Inserting this into Eq. (14) and taking the trace over the environmental degrees of freedom, we find that the radiation field term can be written in the simple and familiar form (still in the variational representation interaction picture)

$$\tilde{\mathcal{K}}_{\text{sp}}(\tilde{\rho}_V(t)) = \Gamma(t) \left(\sigma_- \tilde{\rho}_V(t) \sigma_+ - \frac{1}{2} \{ \sigma_+ \sigma_-, \tilde{\rho}_V(t) \} \right). \quad (15)$$

where we ignore absorption and stimulated emission processes under the assumption that no thermal photons exist at the appropriate energy scale for temperatures of interest. Additionally, we have ignored the Lamb-shift of the excitonic energy splitting induced by the radiation field. Importantly, the rate of spontaneous emission processes is given here by

$$\Gamma(t) = 2\text{Re} \int_0^t d\tau e^{i\omega_0 \tau} C(\tau) \sum_{\mathbf{q}} |h_{\mathbf{q}}|^2 e^{-i\eta_{\mathbf{q}} \tau}, \quad (16)$$

where

$$C(\tau) = \exp \left[- \int_0^\infty d\omega \frac{J_{\text{ph}}(\omega)}{\omega^2} F(\omega)^2 ((1 - \cos \omega \tau) \coth \beta \omega / 2 + i \sin \omega \tau) \right], \quad (17)$$

with $f_{\mathbf{k}} = g_{\mathbf{k}} F(\omega_{\mathbf{k}})$, is the usual polaron-type bath correlation function for the phonon operators, i.e. $C(\tau) = \langle B_{\pm}(\tau) B_{\mp}(0) \rangle_{B_1}$, written in the continuum limit, with $J_{\text{ph}}(\omega) = \sum_{\mathbf{k}} |g_{\mathbf{k}}|^2 \delta(\omega - \omega_{\mathbf{k}})$ being the spectral density relevant to the phonon bath. Taking the continuum limit for the radiation field in Eq. (16), we can then write the spontaneous emission rate as

$$\Gamma(t) = 2\text{Re} \int_0^t d\tau e^{i\omega_0 \tau} C(\tau) X(\tau), \quad (18)$$

where we define the radiation field correlation function $X(\tau) = \int_0^\infty d\eta e^{-i\eta \tau} J_{\text{pt}}(\eta)$, where $J_{\text{pt}}(\eta) = \sum_{\mathbf{q}} |h_{\mathbf{q}}|^2 \delta(\eta - \eta_{\mathbf{q}})$ is the relevant spectral density for the photon environment. Thus, the spontaneous emission rate we derive within the variational theory is dependent upon both the phonon and photon bath correlation functions, $C(\tau)$ and $X(\tau)$, respectively, and whether this rate varies from that in the absence of the phonon environment depends crucially on their respective timescales.

Consider now the case of no phonon environment, such that we can set $C(\tau) \rightarrow 1$. Then, we have

$$\Gamma_1(t) = 2\text{Re} \int_0^t d\tau e^{i\omega_0 \tau} \int_0^\infty d\eta e^{-i\eta \tau} J_{\text{pt}}(\eta), \quad (19)$$

which, if take the limit of $t \rightarrow \infty$, gives the standard Markovian spontaneous emission rate $\Gamma_1 = 2\pi J_{\text{pt}}(\omega_0)$, dependent upon the photon bath spectral density evaluated at the excitonic energy splitting ω_0 .

Now, consider the opposite limit in which the exciton-phonon interaction is such that the QD polaron states are reached on an extremely short timescale. In this situation, we replace $C(\tau) \rightarrow C(\infty) = B^2$ in Eq. (18), and we then obtain the modified spontaneous emission rate

$$\Gamma' = B^2 \Gamma_1 = 2B^2 \pi J_{\text{pt}}(\omega_0), \quad (20)$$

again within the Markov approximation.

We now return to the full expression for $\Gamma(t)$ in Eq. (18) to determine the appropriate form for the present situation of a coherently-driven driven QD coupled also to an acoustic phonon environment. In this case, we know that the

typical timescale for the phonon-bath correlation function to reach the long-time value of B^2 is of the order of a few picoseconds [13, 14]. For the radiation field correlation function, $X(\tau)$, we take the standard (3D) spectral density $J_{\text{pt}}(\eta) = A\eta^3 e^{-\eta/\eta_c}$, where a high-frequency cut-off η_c has been introduced. This gives

$$X(\tau) = \frac{6A}{(\eta_c^{-1} + i\tau)^4}, \quad (21)$$

which decays to zero on a timescale of roughly $1/\eta_c$. Hence, in the limit of large η_c , this correlation function becomes extremely short-lived [?]. We know that in the present case, η_c must be at least as large as ω_0 (the ground-state to single-exciton state energy splitting), otherwise spontaneous emission would be suppressed. Thus, we can estimate $\eta_c > 1.5 \times 10^3 \text{ ps}^{-1}$, for a typical $|0\rangle$ to $|X\rangle$ energy splitting of 1 eV, which leads to a radiation field correlation time of the order of femtoseconds *at most*. On this timescale, the phonon correlation function barely changes, and we may replace $C(\tau)$ by $C(0) = 1$ in Eq. (18), and we are also now justified in taking the upper limit of integration to infinity for timescales of interest. We therefore conclude that, for a typical QD system described by the Hamiltonian of Eq. (5), the spontaneous emission process is unaltered by the exciton-phonon coupling, and can be described by the standard Lindblad form of Eq. (15) with $\Gamma(t)$ replaced with $\Gamma_1 = 2\pi J_{\text{pt}}(\omega_0)$. We can thus write the full variational frame interaction picture master equation as the sum of two terms

$$\frac{d\tilde{\rho}_V(t)}{dt} = \tilde{\mathcal{K}}_{\text{ph}}(\tilde{\rho}_V(t)) + \Gamma_1 \left(\sigma_- \tilde{\rho}_V(t) \sigma_+ - \frac{1}{2} \{ \sigma_+ \sigma_-, \tilde{\rho}_V(t) \} \right), \quad (22)$$

the first describing exciton-phonon interactions within variational theory, and the second giving rise to spontaneous emission processes.

Phonon coupling terms

Having separated the phonon and photon coupling contributions, we now use the methods described in Ref. [32] to find the form of the phonon terms. The variational parameters upon which H_{1a} , H_{1b} and H_S all depend are found by minimising a free energy bound on the interaction terms. We find $f_{\mathbf{k}} = g_{\mathbf{k}} F(\omega_{\mathbf{k}})$ with

$$F(\omega_{\mathbf{k}}) = \frac{(1 - \frac{\epsilon}{\eta} \tanh(\beta\eta/2))}{1 - \frac{\epsilon}{\eta} \tanh(\beta\eta/2) \left(1 - \frac{\Omega_r^2}{2\epsilon\omega_{\mathbf{k}}} \coth(\beta\omega_{\mathbf{k}}/2) \right)}, \quad (23)$$

and we note that this means the renormalised driving strength,

$$\Omega_r = \Omega \exp \left[-\frac{1}{2} \int_0^\infty \frac{J_{\text{ph}}(\omega)}{\omega^2} F(\omega)^2 \coth(\beta\omega/2) d\omega \right], \quad (24)$$

and $R = \sum_{\mathbf{k}} \omega_{\mathbf{k}}^{-1} f_{\mathbf{k}} (f_{\mathbf{k}} - 2g_{\mathbf{k}})$ must be simultaneously solved for self-consistently.

In the Schrödinger picture, $\dot{\rho}_V(t) = \exp[-iH_S t] \dot{\rho}_V(t) \exp[iH_S t] - i[H_S, \rho_V]$, the phonon terms can be written

$$\begin{aligned} \mathcal{K}_{\text{ph}}(\rho_V(t)) = & -\frac{1}{2} \sum_{ij} \sum_{\omega} \gamma_{ij}(\omega) [A_i, A_j(\omega) \rho_V(t) - \rho_V(t) A_j^\dagger(\omega)] \\ & - i \sum_{ij} \sum_{\omega} S_{ij}(\omega) [A_i, A_j(\omega) \rho_V(t) + \rho_V(t) A_j^\dagger(\omega)], \end{aligned} \quad (25)$$

where $\{i, j\} \in \{1, 2, 3\}$ and $\omega \in \{0, \pm\xi\}$. We define $A_1 = \sigma_x$, $A_2 = \sigma_y$ and $A_3 = (1/2)(I + \sigma_z)$, while $A_1(0) = \sin 2\theta(|+\rangle\langle+| - |-\rangle\langle-|)$, $A_1(\xi) = \cos 2\theta |-\rangle\langle+|$, $A_2(0) = 0$, $A_2(\xi) = i |-\rangle\langle+|$, $A_3(0) = \cos^2 \theta |+\rangle\langle+| + \sin^2 \theta |-\rangle\langle-|$ and $A_3(\xi) = -\sin \theta \cos \theta |-\rangle\langle+|$, defined in terms of the eigenstates of H_S , satisfying $H_S |\pm\rangle = (1/2)(R \pm \xi) |\pm\rangle$. In all cases $A_i(\omega) = A_i^\dagger(-\omega)$. The angle $\theta = (1/2) \arctan(\Omega_r/\epsilon)$ characterises the tilt of the system eigenstates away from the x -axis in the variational frame. Eq. (25) contains the quantities $\gamma_{ij}(\omega) = 2\text{Re}[K_{ij}(\omega)]$ and $S_{ij}(\omega) = \text{Im}[K_{ij}(\omega)]$, defined in terms of the response functions

$$K_{ij}(\omega) = \int_0^\infty \Lambda_{ij}(\tau) e^{i\omega\tau} d\tau, \quad (26)$$

which themselves depend on the bath correlation functions $\Lambda_{ij}(\tau) = \text{Tr}(\tilde{B}_i(\tau)\tilde{B}_j(0)\rho_B)$. Note that in Eq. (26) we have extended the upper limit of integration to infinity which, for the parameters considered in the main text, is a good approximation [28]. We label the bath operators $B_1 = (\Omega/2)B_x$, $B_2 = (\Omega/2)B_y$, and $B_3 = \sum_{\mathbf{k}}(g_{\mathbf{k}} - f_{\mathbf{k}})(b_{\mathbf{k}}^\dagger + b_{\mathbf{k}})$. The bath correlation functions are found to be $\Lambda_{11}(\tau) = (\Omega_r^2/8)(e^{\phi(\tau)} + e^{-\phi(\tau)} - 2)$ and $\Lambda_{22}(\tau) = (\Omega_r^2/8)(e^{\phi(\tau)} - e^{-\phi(\tau)})$, with phonon propagator

$$\phi(\tau) = \int_0^\infty d\omega \frac{J(\omega)}{\omega^2} F(\omega)^2 G_+(\tau), \quad (27)$$

defined in terms of $G_\pm(\tau) = (n(\omega) + 1)e^{-i\omega\tau} \pm n(\omega)e^{i\omega\tau}$, with $n(\omega) = (e^{\beta\omega} - 1)^{-1}$ the occupation number, while

$$\Lambda_{33}(\tau) = \int_0^\infty d\omega J(\omega)(1 - F(\omega))^2 G_+(\tau), \quad (28)$$

$$\Lambda_{32}(\tau) = \frac{\Omega_r}{2} \int_0^\infty d\omega \frac{J(\omega)}{\omega} F(\omega)(1 - F(\omega))iG_-(\tau), \quad (29)$$

with $\Lambda_{32}(\tau) = -\Lambda_{23}(\tau)$, and $\Lambda_{12}(\tau) = \Lambda_{21}(\tau) = \Lambda_{13}(\tau) = \Lambda_{31}(\tau) = 0$.

Putting everything together, we arrive at the full variational frame Schrödinger picture master equation

$$\frac{d\rho_V(t)}{dt} = -\frac{i}{2}[\epsilon\sigma_z + \Omega_r\sigma_x, \rho_V(t)] + \mathcal{K}_{\text{ph}}(\rho_V(t)) + \Gamma_1 \left(\sigma_- \rho_V(t) \sigma_+ - \frac{1}{2} \{ \sigma_+ \sigma_-, \rho_V(t) \} \right), \quad (30)$$

as used in the main text. We note that in moving the spontaneous emission terms back into the Schrödinger picture the QD operators σ_\pm have remained unchanged to be consistent with the approximation leading to Eq. (11). Making use of the quantum regression theorem in the standard way, Eq. (30) can then be used to calculate the field correlation properties of the QD. Slight care must be taken, however, when relating QD expectation values in the variational frame to those in the original frame. If χ and χ_V are the original and variational frame total density operators, respectively, we have $\text{tr}_{S+B}[\chi\sigma_z] = \text{tr}_{S+B}[e^{-V}\chi_V e^V\sigma_z] = \text{tr}_{S+B}[\chi_V\sigma_z]$. However, for $n = x, y$, we have $\text{tr}_{S+B}[\chi\sigma_n] = \text{tr}_{S+B}[e^{-V}\chi_V e^V\sigma_n] = B\text{tr}_{S+B}[\rho_V\sigma_n]$ where we have made a Born approximation in the variational frame, $\chi_V \approx \rho_V\rho_B$.

Pure-dephasing limit

Though we use Eq. (25) to numerically calculate the field correlation properties of the QD, the analytical expressions resulting from it are somewhat cumbersome. However, in the correct (weak-driving) limit, we find that the phonon coupling terms in Eq. (25) can be well approximated by a simple pure dephasing form. Assuming now that we drive the QD on resonance with the polaron shifted transition frequency, $\nu - \sum_{\mathbf{k}} \omega^{-1} g_{\mathbf{k}}^2 = 0$, and we drive weakly enough such that $\Omega \ll \omega_c$, then the variational transformation reduces approximately to the full polaron form, and we can thus set $F(\omega_{\mathbf{k}}) \approx 1$ in Eq. (23). As such, we find that only the correlation functions $\Lambda_{11}(\tau)$ and $\Lambda_{22}(\tau)$ survive, and the variational master equation [Eq. (25)] reduces to the polaron form given in Ref. [28]. This corresponds to Bloch equations of the form $\dot{\boldsymbol{\alpha}} = \mathbf{M} \cdot \boldsymbol{\alpha} + \mathbf{b}$ where

$$\mathbf{M} = \begin{pmatrix} -(\Gamma_z - \Gamma_y) & 0 & 0 \\ 0 & -\Gamma_y & -\Omega_r \\ 0 & (\Omega_r + \lambda) & -\Gamma_z \end{pmatrix}, \quad (31)$$

and $\mathbf{b} = (-\kappa_x, 0, 0)^T$, with Bloch vector $\boldsymbol{\alpha} = (\langle\sigma_x\rangle_t, \langle\sigma_y\rangle_t, \langle\sigma_z\rangle_t)^T$. Here, the rates and energy shifts are given by

$$\Gamma_y = 2\gamma_{11}(0), \quad (32)$$

$$\Gamma_z = (\gamma_{22}(\Omega_r) + \gamma_{22}(-\Omega_r) + 2\gamma_{11}(0)), \quad (33)$$

$$\lambda = 2(S_{22}(\Omega_r) - S_{22}(-\Omega_r)), \quad (34)$$

$$\kappa = (\gamma_{22}(\Omega_r) - \gamma_{22}(-\Omega_r)). \quad (35)$$

We are interested in the solutions to these Bloch equations for arbitrary initial conditions as, with the help of the regression theorem, this will fully determine the first-order field correlation function and hence the QD emission

spectrum. We find that the solutions to the Bloch equations can be written

$$\langle \sigma_x \rangle_t = \frac{e^{-(\Gamma_z - \Gamma_y)t}}{\Gamma_z - \Gamma_y} [\langle \sigma_x \rangle_0 (\Gamma_z - \Gamma_y) + \kappa] - \frac{\kappa}{\Gamma_z - \Gamma_y}, \quad (36)$$

$$\langle \sigma_y \rangle_t = \frac{e^{-(\Gamma_y + \Gamma_z)t/2}}{2\zeta} [\langle \sigma_y \rangle_0 (2\zeta \cos(\zeta t) + (\Gamma_z - \Gamma_y) \sin(\zeta t)) - 2\Omega_r \langle \sigma_z \rangle_0 \sin(\zeta t)], \quad (37)$$

$$\langle \sigma_z \rangle_t = \frac{e^{-(\Gamma_y + \Gamma_z)t/2}}{2\zeta} [\langle \sigma_z \rangle_0 (2\zeta \cos(\zeta t) - (\Gamma_z - \Gamma_y) \sin(\zeta t)) + 2(\lambda + \Omega_r) \langle \sigma_y \rangle_0 \sin(\zeta t)], \quad (38)$$

where $\zeta = \sqrt{\Omega_r(\lambda + \Omega_r) - (1/4)(\Gamma_z - \Gamma_y)^2}$.

For the appropriate phonon spectral density used in the main text, $J_{\text{ph}}(\omega) = \alpha \omega^3 \exp[-(\omega/\omega_c)^2]$, we find that in the regime that $k_B T < \omega_c$ (equivalently $\beta \omega_c > 1$), as the driving strength becomes small, then $\gamma_{11}(0)$ becomes negligible in comparison to $\gamma_{22}(\pm \Omega_r)$. Hence, $\Gamma_y \rightarrow 0$, while $\Gamma_z \rightarrow (\gamma_{22}(\Omega_r) + \gamma_{22}(-\Omega_r))$. Additionally, $\lambda \ll \Omega_r$ in this regime, and $(\Gamma_z - \Gamma_y)/\zeta \approx \Gamma_z/\sqrt{\Omega_r^2 - (1/4)\Gamma_z^2}$ is very small as well. If we additionally impose $\Omega\beta \ll 1$, such that $\kappa/\Gamma_z \rightarrow 0$, then we may now approximate the Bloch equation solutions as

$$\langle \sigma_x \rangle_t \approx e^{-\Gamma_z t} \langle \sigma_x \rangle_0, \quad (39)$$

$$\langle \sigma_y \rangle_t \approx e^{-\Gamma_z t/2} \left[\langle \sigma_y \rangle_0 \cos(\zeta t) - \frac{\Omega_r}{\zeta} \langle \sigma_z \rangle_0 \sin(\zeta t) \right], \quad (40)$$

$$\langle \sigma_z \rangle_t \approx e^{-\Gamma_z t/2} \left[\langle \sigma_z \rangle_0 \cos(\zeta t) + \frac{\Omega_r}{\zeta} \langle \sigma_y \rangle_0 \sin(\zeta t) \right], \quad (41)$$

where $\zeta \rightarrow \sqrt{\Omega_r^2 - (1/4)\Gamma_z^2}$. Now, if we identify $\gamma_{PD} = \Gamma_z$, then these are precisely the solutions we expect from a simple pure dephasing master equation of the form

$$\dot{\rho} = -\frac{i\Omega_r}{2}[\sigma_x, \rho] + \frac{\gamma_{PD}}{2}(\sigma_z \rho \sigma_z - \rho), \quad (42)$$

in the relevant regime of $\gamma_{PD}/\sqrt{\Omega_r^2 - (1/4)\gamma_{PD}^2}$ being small. Furthermore, if we wish to ensure that the system tends to the correct steady state in the long-time limit, we then need to add a term $(i\kappa/4)[\sigma_y, \{\sigma_z, \rho\}]$ to the right-hand-side of Eq. (42), such that the solution for $\langle \sigma_x \rangle_t$ becomes $\langle \sigma_x \rangle_t = \frac{e^{-\Gamma_z t}}{\Gamma_z} [\langle \sigma_x \rangle_0 \Gamma_z + \kappa] - \frac{\kappa}{\Gamma_z}$. This justifies the forms given in the main text for weak driving, and is further confirmed by the agreement we see with the full numerical solution of the variational master equation in the appropriate regimes.